"Elapsed times" in Monte Carlo simulations for strongly coupled classical one-component plasmas

Shuji Ogata and Setsuo Ichimaru
Department of Physics, University of Tokyo, Bunkyo, Tokyo 113, Japan
(Received 9 February 1988)

The microscopic features of the particle trajectories in the Monte Carlo (MC) simulations of strongly coupled one-component plasmas are analyzed as functions of the sequential number c of the MC configurations. It is found that the MC particles behave as if they were trapped in the potential dimples of ion spheres in the small-c regime; in the large-c regime they perform diffusive motion in the fluid simulations and remain localized around the lattice sites in the crystalline simulations. These findings enable us to establish a correspondence between c and the "MC elapsed time." Application of this correspondence in the large-c regime leads to an estimate of the diffusion coefficient in the fluid regime which agrees well with the one evaluated independently through the molecular-dynamics method.

I. INTRODUCTION

The classical one-component plasma[1] (OCP) is a system consisting of charged particles of a single species, with electric charge Ze, number density n, and temperature T, embedded in a uniform neutralizing background of opposite charges. The state of such a system can be characterized by the Coulomb coupling constant $\Gamma=(Ze)^2/ak_BT$, the inverse temperature in units of the average Coulomb energy, where $a=(4\pi n/3)^{-1/3}$ is the ion-sphere radius. In this paper we shall henceforth scale all the lengths in units of a, unless specified otherwise.

Equilibrium properties of the strongly coupled (i.e., $\Gamma\gg 1$) OCP have been studied extensively through the Monte Carlo[2-5] (MC) and molecular-dynamics[6] (MD) simulation methods. It has been predicted on the basis of MC calculations that the OCP undergoes a first-order freezing transition (i.e., Wigner crystallization) into a bcc crystalline state at $\Gamma_m=178\pm 1$ (Ref. 4) or $\Gamma_m=180\pm 1$ (Ref. 5). Since the transition is of the first order, there is a possibility that the OCP may make a glass transition[7] through a supercooled fluid state if a sufficiently "rapid quench" is applied to the system.[8]

In the computer-simulation studies of the phase evolution in ordinary substances, one resorts to MD methods at constant temperature and pressure;[9,10] the scheme of microcanonical MD simulation needs adequate modifications, however, to accommodate such a condition. The MC methods, on the other hand, can naturally incorporate isothemal and/or isobaric conditions with the appropriate energy and/or volume fluctuations. The situation is simplified further in the cases of the OCP, since the volume fluctuations vanish automatically due to the presence of the uniform background of neutralizing charges.

The major shortcoming of the MC method in the phase-evolution study is an apparent lack of the "time" concept. In this paper, to find a way to circumvent such a shortcoming, we perform several series of MC runs for strongly coupled ($\Gamma\geq 80$) OCP's both in the fluid and in the crystalline states, and thereby analyze the microscopic features of the MC trajectories as functions of the sequential number of the MC configurations (denoted as c). We shall thus find that the MC particles behave as if they are trapped in the potential dimples of the ion spheres in the small-c regime ($c/N<10^2$), where N is the number of MC particles; in the large-c regime ($c/N>10^3$), they perform diffusive motion in the fluid simulations, and remain localized around the lattice sites in the crystalline simulations. We then carry out MC-simulation analysis of Brownian particles in a dimple of the ion-sphere potential, which enables us to find a correspondence between c/N and the "MC elapsed time" t. Application of this correspondence in the large-c regime leads to an estimate of the diffusion coefficient in the fluid regime, which agrees well with the one evaluated independently through the MD simulation method.[6]

II. MONTE CARLO TRAJECTORIES

We have performed MC simulations of various cases of strongly coupled OCP's following the standard Metropolis algorithm, as before.[4,5] In so doing we have introduced three different schemes of particle displacements with the following probability functions:

$$P(r)=(2\Gamma/\pi)^{1/2}(\Gamma r^2)\exp(-\Gamma r^2/2) \tag{1}$$

(scheme A),

$$P(r)=(2\Gamma/\pi)^{1/2}\exp(-\Gamma r^2/2) \tag{2}$$

(scheme B). In either case $P(r)$ is normalized so that

$$\int_0^\infty dr\,P(r)=1\ .$$

In addition, we have scheme C where a particle displacement $\Delta\mathbf{r}=(\Delta x,\Delta y,\Delta z)$ takes place with equal probability in a cube: $|\Delta x|\leq\delta$, $|\Delta y|\leq\delta$, $|\Delta z|\leq\delta$. Here the Cartesian axes are along the MC-cell axes, and δ is

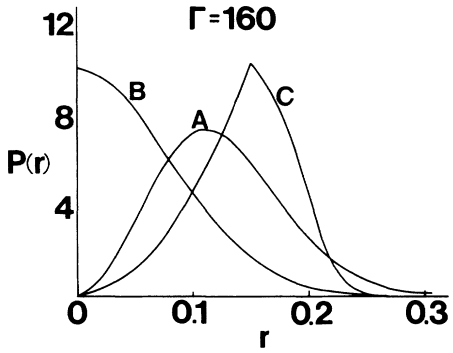

FIG. 1. Displacement probabilities for schemes A, B, and C at $\Gamma=160$. Lengths (e.g., r) are measured in units of the ion-sphere radius, $a=(4\pi n/3)^{-1/3}$.

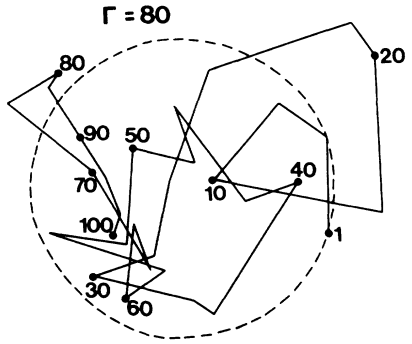

FIG. 2. Trajectories of a MC particle over 100 configurations (per particle) projected onto the x-y plane for scheme A at $\Gamma=80$. The position of the particle is marked with a closed circle at every ten configurations. The dashed circle depicts a sphere with radius $(3/\Gamma)^{1/2}$.

chosen so that the acceptance ratio of the MC runs lies between 0.3 and 0.7. In practice we have chosen $\delta=0.2$ for $\Gamma=80$ and $\delta=0.15$ for $\Gamma=120$ and 160.

In Fig. 1 we depict those three displacement probabilities at $\Gamma=160$ as functions of r. Schemes A and B retain rotational invariance, while scheme C is the one which has been used conventionally.[2-5] Mean-square displacements of the schemes A, B, and C are $3/\Gamma$, $1/\Gamma$, and δ^2, respectively.

In those three schemes we have performed several runs of MC simulations for combinations of Γ and N; the durations of the MC runs are $4-7\times10^6$ configurations.

In Figs. 2–6, we depict trajectories of a MC particle over 100–160 configurations (per particle) projected onto the x-y plane for various cases of the MC runs. We have found that in such a short "interval" the particle motion is confined more or less within a sphere of radius $(3/\Gamma)^{1/2}$, the dashed circle drawn in each figure for comparison, irrespective of the schemes of displacements.

Such a confined motion of a particle may be correlated with the single-particle behavior in the dimple ($r<1$) of the ion-sphere (IS) potential,

$$\frac{U_{\rm IS}}{k_BT}=-\frac{9}{10}\Gamma+\frac{\Gamma}{2}r^2 . \tag{3}$$

The mean-square displacement of a particle in this dimple is given by $3/\Gamma$; this model is thus valid only for $\Gamma\gg3$.

III. BROWNIAN MOTION IN THE DIMPLE OF THE ION-SPHERE POTENTIAL

The Brownian motion of a single particle in the dimple of the ion sphere may be analyzed through the generalized Langevin equation[11]

$$\frac{d^2\mathbf{r}}{dt^2}=-\xi\frac{d\mathbf{r}}{dt}+\mathbf{A}(t)-\omega^2\mathbf{r} , \tag{4}$$

with

$$\omega^2=\omega_p^2/3=\Gamma k_BT/m . \tag{5}$$

Here $\mathbf{A}(t)$ represents the fluctuating random force and ξ is the microscopic rate of momentum transfer or the friction coefficient.

Under the assumption that the particle is initially located at the origin with Maxwellian velocity distribution, Eq. (4) may be solved as[11]

$$\langle\langle r^2\rangle\rangle=3/\Gamma-(3/\Gamma)\exp[-2(3/\pi\Gamma)^{1/2}\omega_pt]\{\cos[(\tfrac{1}{3}-\xi^2/4\omega_p^2)^{1/2}\omega_pt]+(4\omega_p^2/3\xi^2-1)^{-1/2}\sin[(\tfrac{1}{3}-\xi^2/4\omega_p^2)^{1/2}\omega_pt]\}^2 \quad \text{for } \xi<(4/3)^{1/2}\omega_p , \tag{6}$$

$$\langle\langle r^2\rangle\rangle=3/\Gamma-(3/\Gamma)\exp[-2(3/\pi\Gamma)^{1/2}\omega_pt]\{\cosh[(-\tfrac{1}{3}+\xi^2/4\omega_p^2)^{1/2}\omega_pt]+(1-4\omega_p^2/3\xi^2)^{-1/2}\sinh[(-\tfrac{1}{3}+\xi^2/4\omega_p^2)^{1/2}\omega_pt]\}^2 \quad \text{for } \xi>(4/3)^{1/2}\omega_p . \tag{7}$$

TABLE I. Self-diffusion coefficients obtained in the present simulations with the displacement schemes A, B, and C and those evaluated in the MD simulations (Ref. 6).

	Scheme A	Scheme B	Scheme C		
Γ	($N=1024$)	($N=1024$)	($N=1024$)	($N=432$)	MD
80	0.0070		0.0088	0.0056	0.0083±0.0017
120			0.0038	0.0028	0.0048±0.0010
160	0.0021	0.0025	0.0021	0.0014	0.0033±0.0007

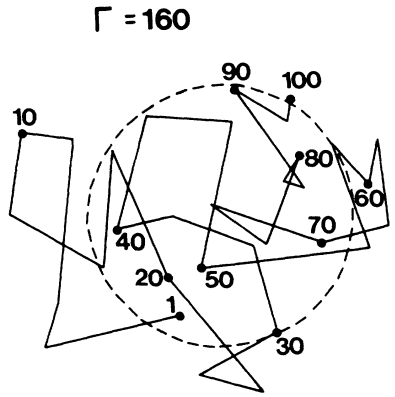

FIG. 3. Same as Fig. 2, but at $\Gamma = 160$.

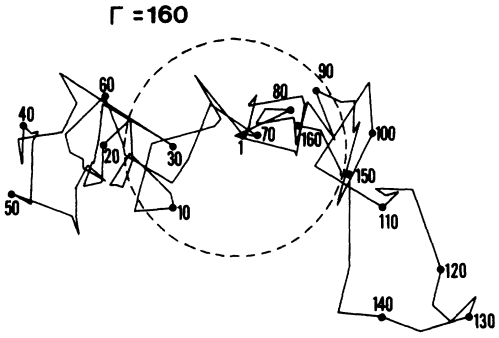

FIG. 4. Same as Fig. 2, but over 160 configurations for scheme B at $\Gamma = 160$.

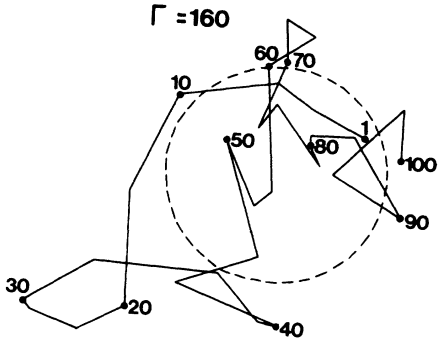

FIG. 5. Same as Fig. 2, but for scheme C at $\Gamma = 160$.

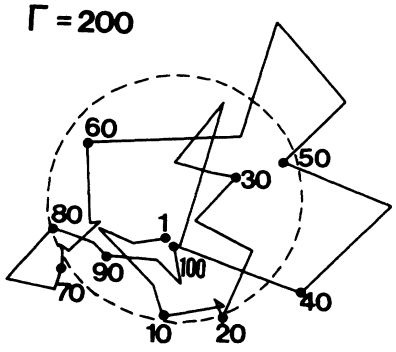

FIG. 6. Same as Fig. 2, but for scheme A at $\Gamma = 200$ in the bcc crystalline state.

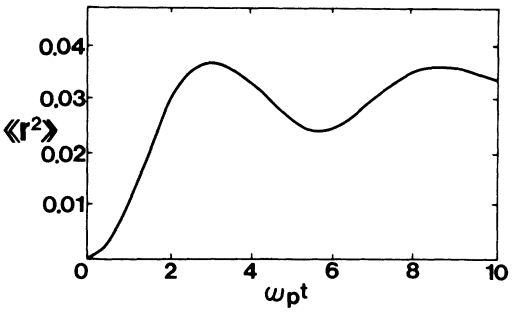

FIG. 7. Double average of r^2 in Eq. (6), at $\Gamma = 80$ with $\xi = 2\omega_p(3/\pi\Gamma)^{1/2} \simeq 0.219\omega_p$, as a function of $\omega_p t$.

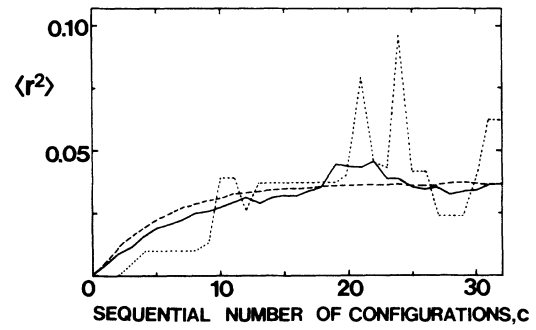

FIG. 8. Brownian motion of a MC particle in the ion-sphere potential Eq. (3), at $\Gamma = 80$ for scheme A, with the initial condition $r = 0$. The dotted line describes a one-particle behavior; the solid line, the average over 10^2 particles; the dashed line, the average over 10^3 particles.

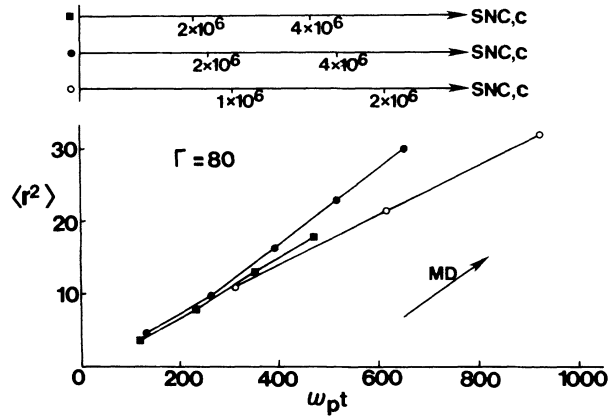

FIG. 9. Mean-square displacement $\langle r^2 \rangle$ of the MC particles in the large-c regime as a function of $\omega_p t$ at $\Gamma = 80$. Closed squares correspond to scheme A with $N = 1024$; closed circles, scheme C with $N = 1024$; open circles, scheme C with $N = 432$. Sequential numbers of configurations in those respective cases are also shown along (SNC,c). For comparison, the value of the slope, $D^* = 2.95\Gamma^{-1.34}$ (Ref. 6), is depicted by the arrow.

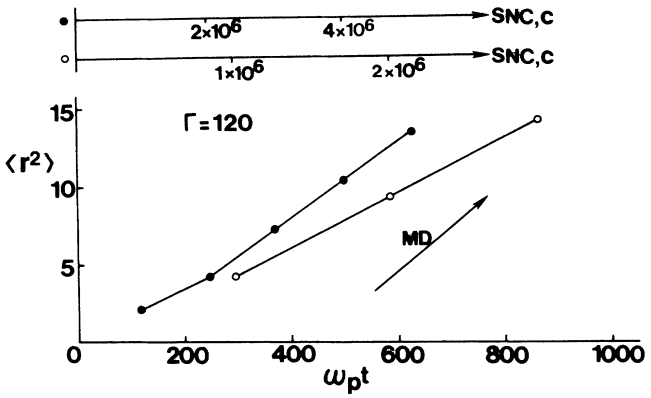

FIG. 10. Same as Fig. 9, but at $\Gamma=120$.

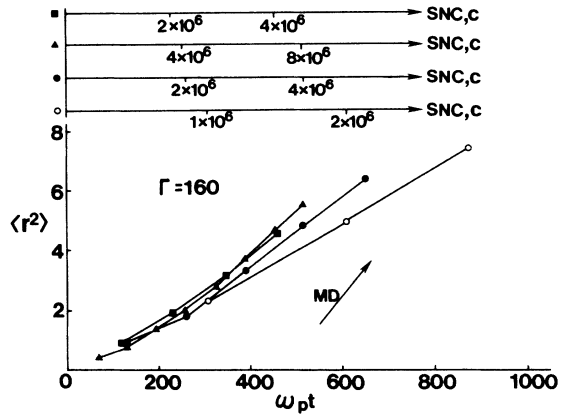

FIG. 11. Same as Fig. 9, but at $\Gamma=160$; the closed triangles correspond to scheme B with $N=1024$.

Here $\langle\langle\ \rangle\rangle$ refers to a double average over single-particle processes and over the Maxwellian distribution.[11] Assuming the ion-sphere model where, $\xi\simeq 2\omega_p\alpha^2(3/\pi\Gamma)^{1/2}$ with $\alpha=1$ (Ref. 1), we find that Eq. (6) applies since $\xi\ll(\frac{4}{3})^{1/2}\omega_p$ and that $\langle\langle r^2\rangle\rangle$ exhibits a peak structure as depicted in Fig. 7 ($\xi=0.219\omega_p$). The peak corresponds to a point of reflection where the particle starting outward from $r=0$ turns over inward. The first peak takes place at $\omega_p t=(\frac{3}{4})^{1/2}\pi$.

We have carried out MC simulations of Brownian motion in the ion-sphere potential (3), starting from $r=0$, at several values of Γ for schemes A, B, and C of displacements. In all the cases, if we average r^2 over a number of particles less than 10, the resulting $\langle r^2\rangle$ appears too noisy for a peak to be identified. If the average is carried out over 10^2 particles, $\langle r^2\rangle$ shows a peak structure. If on the other hand we average r^2 over 10^3 particles or more, the resulting $\langle r^2\rangle$ shows no oscillatory behaviors. This stems from the nature of the MC simulation in that the thermal average with respect to velocities is performed virtually at every step. So if we average r^2 over so many particles, the effective rate of momentum transfer increases, resulting in nonoscillatory behavior of Eq. (7).

Figure 8 illustrates those cases at $\Gamma=80$ in scheme A. Adopting a heuristic approach, we pick the peak observed with an average over 10^2 particles and identify it as the first peak in Fig. 7; we may thereby establish a relationship between $\omega_p t$ and the sequential number of configurations applicable to the MC simulations of strongly coupled OCP's. Sequential numbers of configurations per particle c/N corresponding to the MC time of $\omega_p t=(3/4)^{1/2}\pi$ are thus obtained as follows: scheme A, 23.0±0.8; scheme B, 41.2±1.7; scheme C, 20.5±0.8 ($\Gamma=80$), 21.6±0.8 ($\Gamma=120$), 20.4±0.7 ($\Gamma=160$).

IV. BROWNIAN MOTION IN A STRONGLY COUPLED OCP

As we have seen in Sec. III, MC particles in a strongly coupled OCP behave as if they were trapped in the potential dimples of ion spheres in the small-c regime, $c/N<10^2$. This finding has been used to establish a correspondence between c/N and the MC time in Sec. III. In this section, we analyze simulation results of the mean-square displacements $\langle r^2\rangle$ of the MC particles in the large-c regime, and deduce the coefficient of self-diffusion in light of the correspondence mentioned above.

In Figs. 9–11, we exhibit MC results as functions of $\omega_p t$ for various cases of simulations. For comparison, we depict in those figures the values of the slopes,

$$D^*=\langle r^2\rangle/6\omega_p t=2.95\Gamma^{-1.34} \tag{8}$$

predicted by Hansen *et al.*[6] through their MD simulation studies within errors of 20% applicable for $\Gamma\leq 152.4$. Table I lists and compares the values of the self-diffusion coefficients obtained for $\omega_p t>200$ in various displacement schemes and those of Eq. (8). We find that the present estimates, regardless of the displacement schemes, agree well with the MD results. This fact again corroborates the validity of the MC time concept elucidated in this paper.

[1]See, e.g., S. Ichimaru, *Plasma Physics: An Introduction to Statistical Physics of Charged Particles* (Benjamin/Cummings, Menlo Park, CA, 1986).
[2]S. G. Brush, H. L. Sahlin, and E. Teller, J. Chem. Phys. **45**, 2102 (1966).
[3]J. P. Hansen, Phys. Rev. A **8**, 3096 (1973).
[4]W. L. Slattery, G. D. Doolen, and H. E. DeWitt, Phys. Rev. A **21**, 2087 (1980); **26**, 2255 (1982).
[5]S. Ogata and S. Ichimaru, Phys. Rev. A **36**, 5451 (1987).
[6]J. P. Hansen, I. R. McDonald, and E. L. Pollock, Phys. Rev. A **11**, 1025 (1975); M. Baus and J. P. Hansen, Phys. Rep. **59**, 1 (1980).
[7]S. Ichimaru and S. Tanaka, Phys. Rev. Lett. **56**, 2815 (1986); S. Tanaka and S. Ichimaru, Phys. Rev. A **35**, 4743 (1987).
[8]S. Ogata and S. Ichimaru (unpublished).
[9]H. C. Andersen, J. Chem. Phys. **72**, 2384 (1980).
[10]S. Nosé, Mol. Phys. **52**, 255 (1984); J. Chem. Phys. **81**, 511 (1984).
[11]S. Chandrasekhar, Rev. Mod. Phys. **15**, 1 (1943).